PERGAMON

Available online at www.sciencedirect.com

SCIENCE DIRECT®

Electrochimica Acta 48 (2003) 1263–1271

ELECTROCHIMICA Acta

www.elsevier.com/locate/electacta

Extending surface Raman spectroscopy to transition metals for practical applications IV. A study on corrosion inhibition of benzotriazole on bare Fe electrodes

J.L. Yao [a], B. Ren [a], Z.F. Huang [a], P.G. Cao [b], R.A. Gu [b,*], Zhong-Qun Tian [a,*]

[a] *State Key Laboratory for Physical Chemistry of Solid Surfaces, Department of Chemistry, Xiamen University, Xiamen 361005, People's Republic of China*

[b] *Department of Chemistry, Suzhou University, Suzhou 215006, People's Republic of China*

Abstract

The emphasis in the present study was placed on developing Raman spectroscopy into a versatile technique, which offers an opportunity for investigating the inhibition effect on the corrosion process of bare Fe surfaces. Several surface pretreatments have been developed to bare Fe electrodes in order to obtain a surface of optimal surface-enhanced Raman scattering (SERS). It has been shown that the surface enhancement factor (SEF) of a bare Fe electrode can reach about two to three orders, depending on the roughening procedure. Therefore, SERS can be extended successfully to study some Fe electrode systems of practical importance. Here we present a study on the film formation process and inhibition effect of benzotriazole (BTA) on Fe surfaces. The results show that BTA interacts with Fe surface through its two N atoms of the triazole ring and surface complex polymer of $[Fe_n(BTA)_p]_m$ is formed, which may suppress the dissolution and oxidation of Fe effectively. In addition, the solution pH, the synergetic effect of I^- with BTA was revealed to have a significant influence on the inhibition efficiency.

© 2003 Elsevier Science Ltd. All rights reserved.

Keywords: Surface Raman spectroscopy; Iron; Benzotriazole; Corrosion; Inhibition

1. Introduction

Iron is probably one of the most important and widely used materials, and plays a central role as basic material for the metallurgical industries. The corrosion and passivation behaviour of iron are quite general and important phenomena in the chemical engineering industry and our daily life. Therefore, there is great economical incentive in developing methods and materials to alleviate corrosion [1], which conies only from a good understanding of the mechanisms and processes involved in this complex phenomenon. So far, a wide variety of electrochemical, surface analytical and spectroscopic techniques have been employed in investigating corrosion and inhibition processes on the metal surfaces, which led to huge amount of experimental information available in the literature and to many articles giving extensive review from various aspects [2–4]. Although great efforts have been made, a better understanding of the mechanism of inhibition for corrosion at the molecular level is still to be achieved.

The application of the above-mentioned techniques to present systems have various individual disadvantages. For example, conventional electrochemical techniques can only provide average information on the electrochemical processes occurring at the metal/solution interface at the macroscopic level. Recently, with the fast development of local electrochemical techniques with different lateral resolutions, scanning probe microscopies, such as scanning tunneling microscopy (STM), atomic force microscopy (AFM) and scanning electrochemical microscopy (SECM), have found their wide application in the corrosion science [5]. However, beside the surface morphological information, these techniques can hardly obtain information concerning the interaction between the molecule and the surface. Thus, it is very difficult for them to reveal the inhibition mechanism at the molecular level. On the other hand, the metal

---

* Corresponding authors. Tel.: +86-592-218-1906; fax: +86-592-208-5349.

E-mail address: zqtian@xmu.edu.cn (Z.-Q. Tian).

0013-4686/03/$ - see front matter © 2003 Elsevier Science Ltd. All rights reserved.
doi:10.1016/S0013-4686(02)00834-4

surface used in these techniques is required in general to be of smooth surface or a mild roughness. This prerequisite is not suitable for many electrodes for the practical application as they have high surface roughness.

By contrast, although the spatial resolution of the spectroscopic techniques was low, some of them were capable of investigating the interface microscopically at the molecular level and provided the useful and complementary information. There have been significant developments in vibrational spectroscopies that have some advantages in monitoring inhibition mechanisms at the molecular level. Among them, IR and Raman spectroscopies are two of the widely used techniques in the electrochemical system. IR has made great contributions in spectroelectrochemistry to reveal the nature of the adsorbed species on a metal surface with high surface reflectivity, such as single crystal electrodes, smooth polycrystalline electrodes or surfaces of mild roughness, which greatly limited itself in the practical application [6–9].

Conventional Raman technique has no enough sensitivity to investigate the interaction of inhibitors as submonolayer adsorbate with a metal surface. However, surface-enhanced Raman spectroscopy (SERS) has extremely high surface sensitivity, which makes it feasible to investigate in situ the monolayer adsorption on metal electrodes. Unfortunately, in the past two decades, the application of this technique has been restricted almost entirely to Ag, Au and Cu, on which the most pronounced SERS effect exists [10–15]. This has impeded the wider application of Raman spectroscopy in surface science and electrochemical process at Fe-group surfaces. As a consequence, corrosion specialists have never been able to study in situ the inhibition processes by surface Raman spectroscopy directly on a bare Fe electrode. However, they made great efforts to extend SERS studies to Fe-group metals in the past decades [16–23]. Three approaches as follows were employed to study the corrosion, inhibition and passivation of Fe-group metals.

The first involves coating a SERS active Ag or Au electrode with a very thin overlayer of Fe by electrochemical deposition [16–18]. By use of the long-range enhancement (electromagnetic mechanism) created by the SERS active substrate underneath, the high quality spectra of the inhibitor adsorbed on the metal surface were obtained. However, it is extremely difficult to eliminate entirely the possibility that the adsorbate is bound to the exposed rough substrate rather than to the overlayer sites because the ultra thin film is only one to five atomic monolayers in thickness on a very surface and some residual substrate sites are usually exposed. Weaver and his coworkers developed an electrodeposition method to produce ‘pinhole free’ films on the SERS active Au substrate [24–26]. It is a significant progress compared with what have been reported before. However, in some special situation, which the electrochemical system has to be studied in a very wide potential range and under the rigorous reaction condition, the stability and reversibility of this kind of ultrathin film electrode will be a problem.

For the second approach, Ag islands of SERS activity were deposited on Fe substrates [19–21]. With the aid of the enhancement of Ag, the surface composition around the Ag islands was detected. However, the same difficulty still exists as the first approach in eliminating entirely the possibility of the molecules adsorbed on the Fe surfaces. Moreover, Ag islands only exhibited strong SERS effect in a narrow potential region and it would quench out of this region. Therefore, this was appropriate only for studying the passive film formed at the Fe substrate [19] rather than the adsorption of the inhibitor.

Recently our laboratory reported a third approach to electrochemically deposit a thick Fe film on a non-SERS active substrate such as glassy carbon [22,23], and obtained the high quality surface Raman spectra of pyridine adsorbed on it. This way, at least to some extent, partially overcome the problems of the above approach. However, it should be pointed out that the crystalline structure and properties of these deposited Fe films may not be exactly the same as that of the Fe bulk phase formed by metallurgy. Therefore, it is highly desirable to extend SERS study directly to various processes of corrosion and inhibition occurring on the bulk metal surface.

The most recent progress in surface Raman spectroscopy, especially the very high sensitivity it provides, allows one to gain vibrational information reflecting the adsorbate and substrate interaction from bare transition metal surfaces [27–31]. From the viewpoint of the special interest in corrosion and inhibition of Fe, it is well known that benzotriazole (BTA) is an effective inhibitor for the Fe corrosion. Although the remarkable efficiency of BTA as corrosion inhibitor for Cu and its alloys has been well-documented, little information has been obtained for Fe surfaces. In the present study, with the appropriate roughening procedure developed for Fe surfaces, we are able to obtain the surface Raman spectra of BTA adsorbed on bare Fe electrodes and investigate their inhibition mechanisms.

2. Experimental

Raman spectra were obtained using a confocal microprobe Raman system (LabRam I). The microscope attachment was based on an Olympus BX40 system and used a 50 × long working length objective (8 mm) so that the objective will not be immersed in the electrolyte. A CCD with 1024 × 256 pixels was used as the detector. The sizes of the slit and pinhole in the present study were set at 200 and 800 μm, respectively. The diameter of the laser spot on the electrode is approximately 3 μm. All the experiments were done using the excitation line of 632.8 nm from an internal He–Ne laser with a power of 12 mW on the electrode surface. The working electrode was a polycrystalline Fe disk with a geometric area of 0.1 cm^2 embedded in a Teflon rod. It was polished successively with 0.3 and 0.05 μm alumina slurry (Buehler Ltd.) to a mirror finish, and sonicated in triply distilled water. Careful polishing with finer alumina powder is necessary to obtain homogeneous and SERS-stable roughened Fe surfaces. Various surface-roughening procedures will be described in the following sections. After being roughened, the electrode was rinsed thoroughly and transferred to the spectroelectrochemical cell for measurement. A large Pt ring served as the counter electrode. The reference electrode was a saturated calomel electrode (SCE), thus all the potential quoted here are with respect to SCE. The detailed description on the spectroelectrochemical measurement has been given elsewhere [31]. All experiments were performed at room temperature. All the chemicals used were analytical reagent and the solutions were prepared using Milli-Q water.

3. Results and discussion

3.1. Preparation of roughened Fe electrodes

As has been well known from previous SERS studies on Au, Ag and Cu and the recent studies on Pt and Ni, a necessary requirement for the generation of great surface enhancement is the presence of certain kinds of surface roughness. Five kinds of surface-roughening procedures for Fe electrodes have been investigated in order to obtain a better SERS active surface, (i) mechanical polishing; (ii) chemical etching; (iii) ex situ electrochemical oxidation and reduction cycle (ORC) roughening; (iv) in situ ORC roughening and (v) electrodepositing thin layer of Fe on the massive Fe electrode.

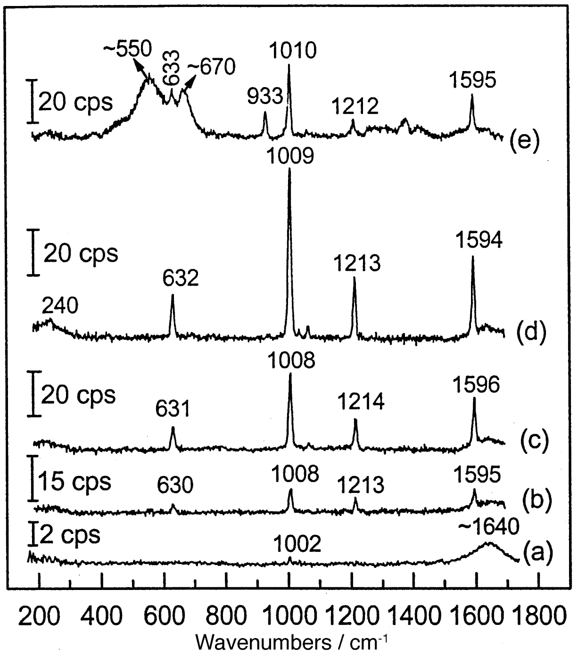

Fig. 1. Raman spectra of pyridine adsorbed on Fe surfaces pretreated using different roughening procedures in a solution containing 0.01 M pyridine and 0.1 M KCl (0.1 M $NaClO_4$ for (e)) at about −0.95 V: (a) mechanically polished; (b) chemically etched in 2 M H_2SO_4; (c) ex situ ORC in 0.5 M H_2SO_4; (d) in situ ORC in 0.01 M pyridine+0.1 M KCl in the spectroelectrochemical cell; and (e) electrodepositing Fe on an iron electrode. The excitation line was 632.8 nm.

Fig. 1 shows a set of Raman spectra of pyridine, as a model molecule in SERS studies, obtained from surface after different surface pretreatments. On comparing the Raman spectra of the adsorbed pyridine from these surfaces, two interesting spectral features should be noted. The first one is the band frequency difference. On the smooth surface, the frequency of the ring breathing vibration (ν_1) mode is almost identical to that of pyridine in the aqueous solution. Therefore, the Raman signal detected comes mostly from the bulk solution. This is contrast to the large shift of the vibrational frequency of the ν_1 mode observed from the roughened Fe surfaces. The second one is the band intensity. Raman signals from the mechanically polished Fe surface are extremely weak to be identified, whilst, those from roughened surfaces could be clearly observed. After the electrode was chemically etched in 2 M H_2SO_4 for 1–2 min, it turned to present a surface of gray colour. At such kind of surface, the signal of the ν_1 mode could reach 8 counts per second (cps). When the electrode was roughened by an ex situ ORC process in 0.5 M H_2SO_4 following the procedures given below, the band intensity of ν_1 increased to about 40 cps with high signal to noise (S/N). The detailed roughening procedure is: the potential was first stepped from −0.7 to −0.35 V and held at −0.35 V for a few seconds. Then the potential was returned to −0.7 V at a slow sweep rate and kept for 1–2 min at the reduction potential to allow the complete electroreduction of the surface oxide layer. If the additional ORC was performed in situ in the spectroelectrochemical cell containing 0.01 M pyridine and 0.1 M KCl prior to the measurement, in which the potential was stepped from −0.7 to −0.05 V where the potential was held for several seconds, and then returned to −0.7 V, the band intensity of the ν_1 increased dramatically to 100 cps. The electrodeposited Fe surface was prepared by depositing a thin layer of Fe onto the mechanical polishing Fe surface in 0.1 M $Fe(NH_4)_2(SO_4)_2$ solution of pH 2.8 at −1.0 V for 30 s. The intensity of the ν_1 mode obtained from this surface is about 40 cps, this band is accompanied by the two bands of medium intensity assigned to the vibration a modes of Fe oxide.

Fig. 1 demonstrates that a proper surface roughening procedure is vitally important to obtain reasonably good spectra for detailed SERS investigation. Based on the spectra of good quality obtained from these surfaces, we are able to estimate the surface enhancement factor (SEF) based on the calculating method developed for the confocal Raman system in our group [32]. The SEF is about two to three orders, depending on the surface roughening procedures.

Although, surface Raman spectra with better S/N could be observed on the last four kinds of surfaces, only the ex situ ORC roughened surface was most suitable to the in situ investigation. The SEF of the chemically polished surface was only half of that of the ex situ ORC roughened surface. In spite of the fact that the SERS intensity is higher for the in situ ORC roughened surface, this surface should be avoided in SERS studies because the adsorbates would be oxidised/reduced or formed surface complex with metal atom (or ion) during the in situ ORC pretreatment. It will make the interpretation of the SERS spectra much more complex. Furthermore, as SERS is very sensitive to the surface species or surface film, the existence of surface iron oxide can be clearly detected. For example, two broad peaks located at about 550 and 670 cm^{-1} are obvious in Fig. 1(e). This surface oxide on the electrodeposited surface will surely influence the adsorption behaviour of the adsorbates, thus it is unsuitable to be used as a SERS substrate.

It should be pointed out that the stability and reversibility of the electrode are two important criteria to select a good surface for both electrochemical and SERS measurements. In order to measure its stability, a set of SERS spectra were recorded in several potential cycles. In each cycle, the electrode potential was first negatively moved and held at the negative potential for about 10 s. Then it was returned to the initial potential. Fig. 2 gives the normalised integrated SERS intensities of the v_1 mode of pyridine adsorbed on the ex situ roughened Fe electrode in each cycle. It is evident from Fig. 2(b) that the signal from Fe electrodes only undergoes slightly decrease at the potential of maximum intensity after a negative potential excursion at −1.2 V. The excursion of the potential in more negative region, such as −1.4 or −1.5 V, will lead to the decrease of the maximum intensity to about 30%, it is still better than the response of typical SERS electrodes (Au and Ag) and much better than Cu. For instance, after the electrode potential was held on the −1.5 V for several seconds, the maximum intensity decreased by 70% for Au electrode and the SERS activity almost quenched for the Ag electrode. This demonstrates a better stability and reversibility of a Fe electrode, if it is prepared properly, compared with typical SERS substrates.

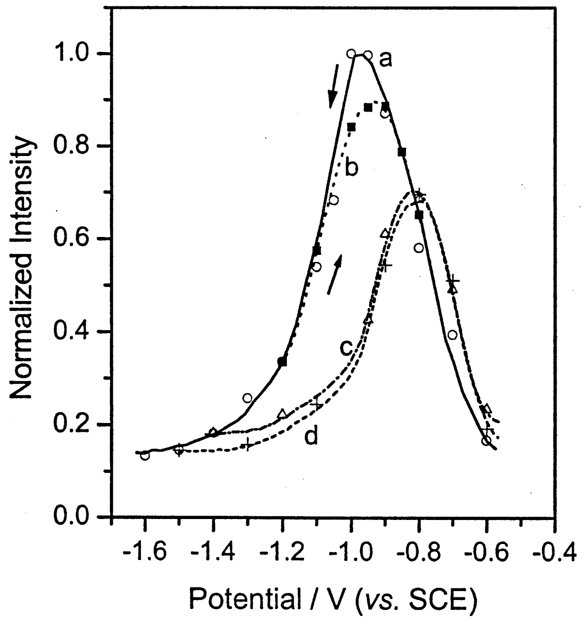

Fig. 2. The integrated intensity–potential profile for the ring breathing mode of pyridine adsorbed on the Fe electrode surface in a solution containing 0.01 M pyridine and 0.1 M KCl. Negatively moved potential (a) and positively moved potential after kept at −1.2 V (b), −1.4 V(c), −1.5V(d), for 10 s.

Furthermore, the ex situ ORC surface is very uniform in terms of morphology. Fig. 3 shows an SEM image of the surface. It shows an even distribution of particles with a size of about 40–60 nm on the surface. Therefore, the surface Raman spectra obtained from a small local region can be representative of the whole surface, which

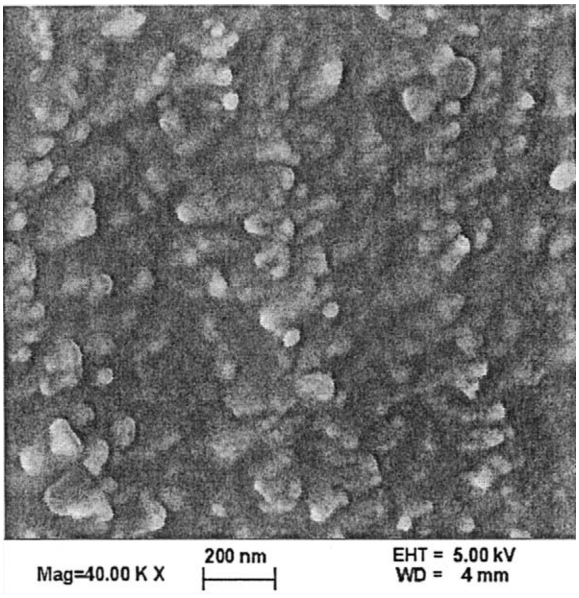

Fig. 3. An SEM image of the ex situ ORC Fe surfaces. Scale bar is shown in the image.

is very important for the interpretation of the experimental findings. It is reasonable to conclude that the ex situ ORC roughened surface can be used as an optimal substrate for both the experimental and practical studies. This kind of surface will allow us to study the corrosion and inhibition processes at massive Fe electrode surfaces at the molecular scale by surface Raman spectroscopy.

3.2. The adsorption of benzotriazole on Fe surfaces

From the viewpoint of the special interest in the corrosion and inhibition of Fe, it is well known that BTA is an effective inhibitor for the metal corrosion. Although the remarkable efficiency of BTA as corrosion inhibitors for Cu and its alloys has been well-documented, little information has been obtained for the Fe surface. It was essential to study its inhibition to the corrosion of Fe in order to achieve a better understanding of its inhibition mechanisms.

Fig. 4 presents a set of potential-dependent SERS spectra of BTA from a roughened Fe electrode together with the normal Raman spectrum of the complex of $\mathrm{Fe}_n\mathrm{BTA}_m$. The potential-dependent spectra were recorded stepwise from the potential at the negative limit to more positive potentials. It can be seen that the SERS intensities change significantly with the applied potentials. This could serve as an evidence that the signal is exactly from the surface species rather than from the bulk solution.

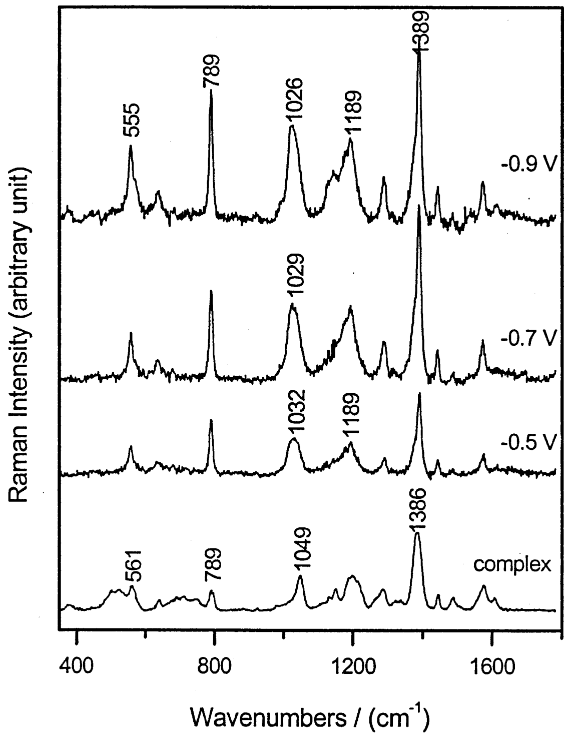

Fig. 4. Normal Raman spectrum of Fe(II)–BTA complex and potential-dependent surface Raman spectra of BTA adsorbed on a Fe electrode in a 0.58 M NaCl solution.

In previous reports, the inhibition mechanisms of BTA for copper mainly involve two types. One is the formation of polymeric complexes with cuprous ion, $[\mathrm{Cu(I)(BTA)}]_n$ [33,34] and another is the adsorption of BTA either in its molecular form of BTAH or in the protonated form of BTAH_2^+ on the Cu surface [35]. The adsorption behaviour depended on the potential, solution pH and the concentration of BTA.

It was very interesting to find that the spectral feature of BTA on Fe in 0.58 M NaCl solution resembles Fe(II)–BTA complex. The assignments of the main bands is listed in the Table 1. For instance, NH in-plane bending mode decreases in intensity greatly and even disappears at more positive potentials. The triazole breathing mode red-shifted by a few wavenumbers after attachment to the surface. Therefore, it indicates that the BTA molecule interacts very possibly with the Fe surface through its triazole ring. Rubim et al. reported that the BTA molecule adsorbed at the Cu surface and formed a surface complex as $[\mathrm{Cu(I)Cl(BTA)}]_n$ [21]. In the present study, the spectral feature of BTA on the Fe surface is similar to that of the Fe and BTA complex. Accordingly, the surface complex $[\mathrm{Fe}_n(\mathrm{Cl})_p(\mathrm{BTA})]_m$ might be formed by the participation of chloride ion and that the adsorption may occur by coordination through the lone pair electrons on a nitrogen atom in the triazole ring with Fe. The formation of surface complex film provided more compact barrier layer leading to a higher inhibition effect.

3.3. pH effect on the film formation behaviour of BTA on Fe

It is well known, the neutral BTA molecule can be protonated by H^+ to form BTAH_2^+ in the acidic solution, while it can also be deprotonated to form BTA^- in the basic solution [36]. This process can be described as follows, $\mathrm{BTA}^- \xleftarrow{\text{base}} \mathrm{BTAH} \xrightarrow{\text{acid}} \mathrm{BTAH}_2^+$. In the neutral solution, it presents in the neutral form. Since the protonation or deprotonation will occur at the triazole ring, it is very possible to probe the existing form of BTA on the metal surface by analysing the changes occurring on the vibrational mode of the triazole ring. Based on these, the pH effect on the film formation was investigated.

Surface Raman spectra of BTA adsorbed on Fe electrodes in solutions of different pH are shown in Fig. 5. After carefully comparing the spectra, one should note the following four points: (i) the feature of the surface Raman spectra obtained in the neutral media is similar to that of Raman spectra of the Fe and BTA complex; (ii) with the decrease of pH, some bands undergo obvious change in intensity. For example, the intensity of the 1189 cm^{-1} band assigned to the

Table 1
Assignments of Raman bands of BTAH solid, BTAH adsorbed on Fe surface and BTA–Fe complex

Solid	SERS (−0.9 V)	$Fe_n(BTA)_m$ complex	Assignments
566	555	561	Triazole ring bend
632	637	640	Triazole ring torsion
780	789	789	Benzene ring breathing
1022	1026	1049	Trizole+benzene ring mode
1096			NH in-plane bend
1126	1122	1133	CH in-plane bending
1146	1150	1150	CH in-plane bending
1207	1190	1201	Triazole ring+NH bending
1280	1288	1286	v Skeletal+CH bending
1385	1389	1387	Benzene+triazole ring stretching
1594	1574	1579	Benzene ring stretching

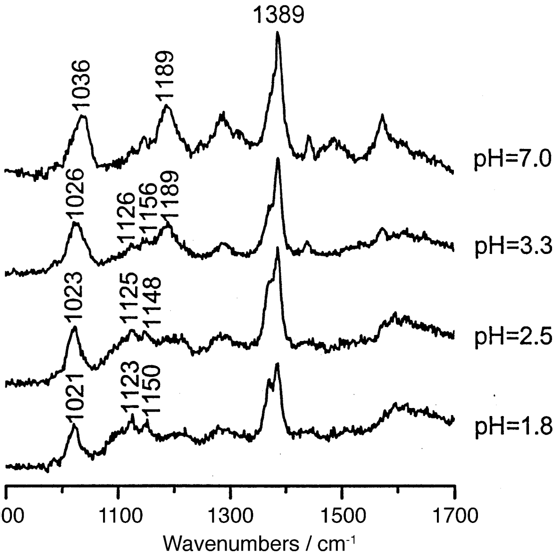

Fig. 5. The pH-dependent surface Raman spectra of BTAH adsorbed at a Fe electrode surface at the potential of −0.6 V.

breathing vibration of the triazole ring decreases remarkably in the solution of low pH, and disappears in the solution of pH 2. The change in the intensity of the ring stretching vibration mode at 1388 cm^{-1} follows the same tendency. However, the intensity of the band at 1126 cm^{-1} attributed to the NH in-plane deformation vibration becomes stronger in the acidic solution; (iii) the frequency of the triazole ring vibrational modes shifts obviously with the change of the solution pH; (iv) the vibrational modes related to the benzene ring decreases in intensity with the decease of the solution pH, which may be related to the special film structure formed between the BTA and the Fe surface.

The similarity of the surface Raman spectra of BTA on Fe surfaces and its complex might provide the evidence that BTA may coordinate with Fe surfaces and form a complex of $[Fe_n(BTA)_p]_m$ in the neutral solution. In such configuration, each Fe atom may coordinate with several BTA^- ions through its N atom. Due to the steric hindrance, some BTA ion can be attached to the surface with their triazole rings, and others with their benzene rings. Therefore, the signal of the vibration mode of benzene ring could be detected in the neutral solution. With the increase in the solution pH, the 1036 cm^{-1} band assigned to the triazole and benzene ring mode red-shifts to 1022 cm^{-1} that is close to the frequency of the free BTAH molecule. It reveals that the structure of surface film of $Fe_n(BTA)_p]_m$ could be destroyed in the acidic solution because of the protonation of the BTA ion. Therefore, the BTA can only adsorb weakly on the surface in its neutral or protonated forms, resulting in the decrease of the inhibition efficiency. No evidence can be found for the formation of the polymer-like film in the acidic solution.

3.4. Synergetic effect of I^- on the inhibition efficiency

It has been well known that, the addition of I^- in the solution will hinder the anodic process, resulting in the

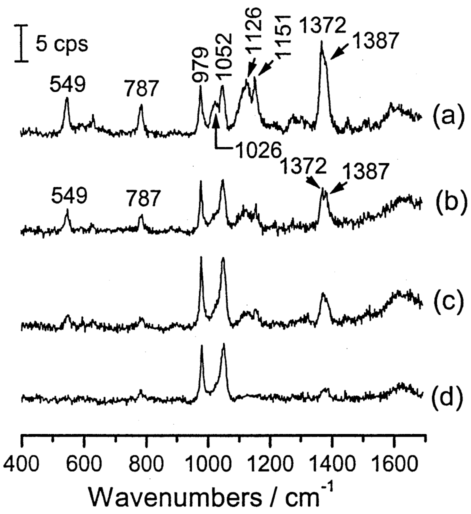

Fig. 6. Surface Raman spectra of BTAH adsorbed on the Fe surface in 0.5 M H_2SO_4 at −0.5 V (a) without KI and with (b) 1×10^{-4} M KI, (c) 5×10^{-4} M Kl and (d) 1×10^{-3} M KI.

positive movement of the corrosion potential. On the other hand, the introduction of BTA to the system, can suppress both the anodic and cathodic processes. However, if I^- and BTA are added into a system, the inhibition effect for both anodic and cathodic processes becomes even more remarkable. It indicates the existence of a synergetic effect between I^- and BTA on the inhibition effect on Fe corrosion. Controversies have been developed to interpret the mechanism of the synergetic effect of these two species [37–40]. The most acceptable three explanations are listed as follows: the first one can be explained by electrostatic adsorption: when a layer of specific adsorbed anion (e.g. halide ions, X^-) adsorbed on a metal surface, the dipole of X–M points to the metal, which is beneficial to the adsorption of the cations from the solution. The second explanation is based on the molecular theory: the improvement of the inhibition effect is due to the covalent bonds formed among the metal substrate, the neutral organic molecules and the anions in the solution, which results in a compact layer over the electrode surface. The third possible mechanism is due to the change of the potential of zero charge (pzc) of the electrode: After the addition of the specifically adsorbed anion, the pzc will be negatively moved, which leads to more adsorbed cations on the surface. It will be very helpful to obtain the information reflecting the interaction between the anion and the organic molecules as well as their interaction with the surface by investigating the synergetic effect of both species.

Fig. 6 presents surface Raman spectra of BTAH adsorbed on the Fe surface in solutions containing I^- of different concentration. For the convenience of comparison, all the Raman spectra were acquired at −0.5 V, and the peaks at 979 and 1052cm^{-1} are from the vibrations of SO_4^{2-} and HSO_4^- of the bulk solution,

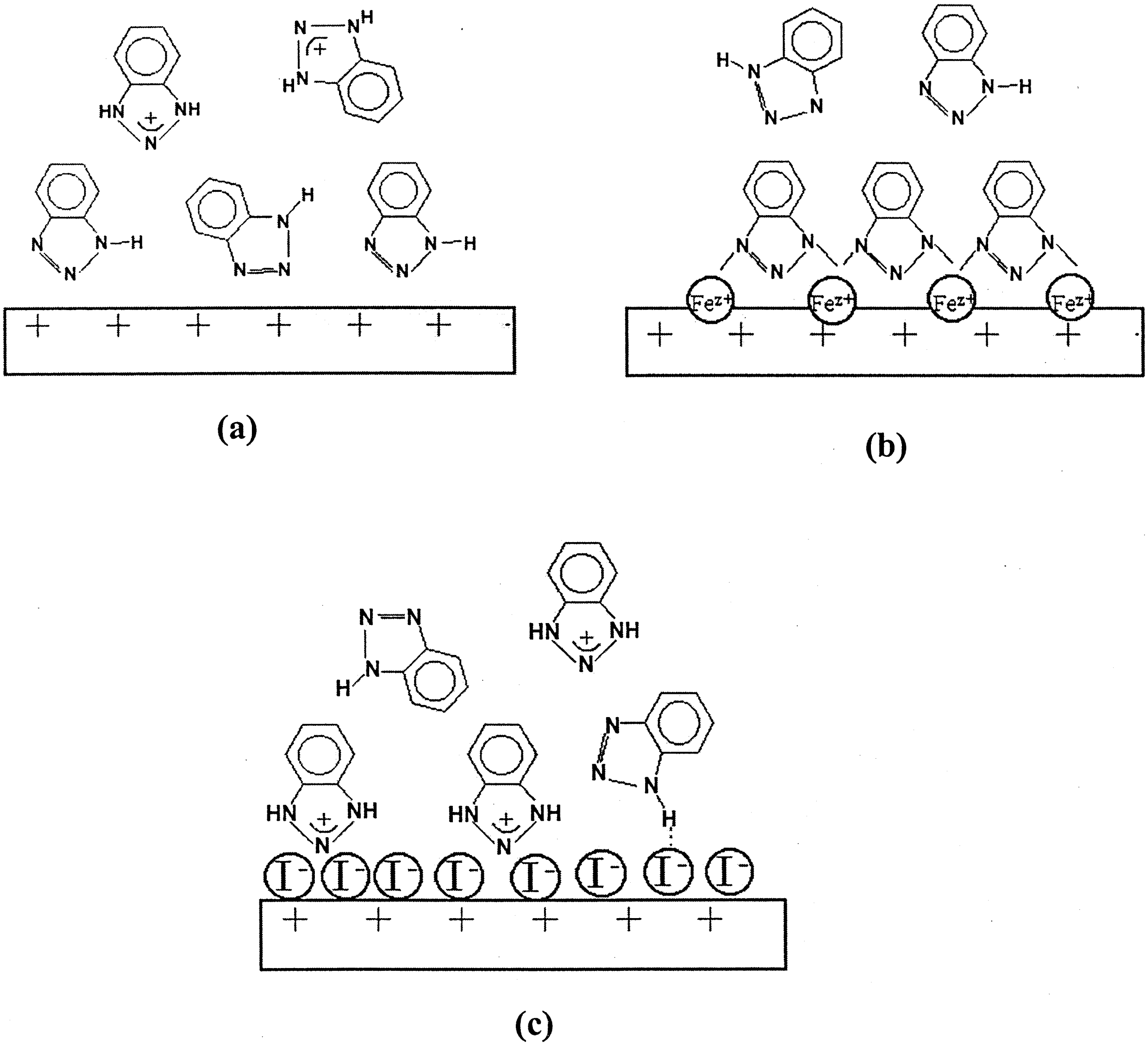

Fig. 7. The adsorption configuration of BTAH on an iron electrode with positive charge in the (a) acidic solution, (b) neutral solution and (c) acidic solution containing I^-.

respectively. The spectral feature from the surface species demonstrates the characteristic vibrations of neutral or protonated form of BTAH. It can be found in the figure that all the intensities of the bands related to BTAH decrease with the addition of I^-. Furthermore, the higher the I^- concentration, the lower the intensities of the BTAH bands. When the I^- concentration is higher than 10^{-3} M, no surface signal from BTAH can be detected. The following three reasons may be responsible for the above phenomenon: (i) The diffusion of BTAH or $BTAH_2^+$ away from the surface after desorption; (ii) the diminish of the SERS activity of the Fe surface; and (iii) possible chemical change of BTAH on the Fe surface resulting in some non-adsorbed species. Since there is no variation on the electrode potential during the addition of I^-, it is very impossible to make the latter two cases happen. Accordingly, one can conclude that in the solution containing I^-, BTAH or $BTAH_2^+$ is replaced by the adsorbed I^- at the surface. As a consequence, there is no direct interaction between the Fe surface and BTAH (or any of its possible existing forms, such as protonated or anion form). Therefore, the enhanced inhibition effect, concerning the synergetic effect is applicable to the present system.

In order to interpret the experimental finding, we proposed three models for Fe in solutions containing different electrolyte, as shown in Fig. 7. In the acidic solution, BTAH adsorbs on the electrode surface in neutral or protonated forms, see Fig. 7(a). There are some water molecules besides BTAH in the adsorbed layer. The addition of specifically adsorbed anions, I^-, will change the composition of the adsorbed layer and replace the BTAH in the layer gradually. The replacement process becomes more facile with the increase of the I^- concentration. In the final stage, an adsorbed I^- layer forms on the Fe surface. $BTAH_2^+$ can then adsorb to the surface through this layer and has no direct interaction with the Fe surface, see Fig. 7(c). There are two major mechanisms that contribute jointly to the SERS: (i) the electromagnetic (EM) enhancement associated with large local fields caused by electromagnetic resonance, and (ii) the chemical enhancement involving a resonance-like Raman process associated with chemical interactions between the molecule and the metal surface. In our case, if the BTA molecule is desorbed and leaves the substrate surface, both of the enhancements, in particular the chemical enhancement, decrease remarkable. As a consequence, the SERS signal of BTA decreases. On the other hand, due to the formation of the adsorbed layer, $BTAH_2^+$ can adsorb more easily on the surface by electrostatic interaction. The synergetic effect of both species results in the improvement in the inhibition efficiency. However, it should be pointed out that not all of the halide ions can induce the synergetic effect with BTAH, e.g. the addition of Cl^- facilitates the anodic dissolution of Fe rather than improving the inhibition efficiency.

4. Conclusions

Several surface roughening procedures for Fe electrodes have been developed and a highly sensitive confocal microprobe Raman system has used. It enables us to in situ obtain high-quality surface Raman spectra of the adsorbed molecules on bare Fe electrodes over a wide applied potential range. The results indicate that the complex polymer film of BTA plays an important role in the inhibition processes of Fe. The synergetic effect of both $BTAH_2^+$ and I^- species results in the improvement in the inhibition efficiency. Through this preliminary study on the inhibition of BTA a roughened Fe electrodes, we have shown the potential of confocal Raman microscopy to be developed as a versatile tool in corrosion science.

Acknowledgements

This work was supported by the Natural Science Foundation of China (299903009, 29833060) and the Ministry of Education of China (99177).

References

[1] C.A. Melendres, N. Camillone, T. Tipton, Electrochim. Acta 34 (1989) 281.

[2] D. Chadwick, T. Hashemi, Corros. Sci. 18 (1978) 39.

[3] Y. Yamamoto, H. Nishihara, K. Aramaki, Corrosion 48 (1992) 641.

[4] C.A. Melendres, in: C. Guiterrez, C. Melendres (Eds.), Spectroscopic and Diffraction Techniques in Interfacial Electrochemistry, Kluwer Academic Publishers, Dordrecht, 1990, pp. 181–222.

[5] E. Kalman, Special issue of trends in corrosion research, Electrochim. Acta 46 (2001) 3607.

[6] B. Beden, C. Lamy, J.-M. Leger, in: J.O.'M. Bockris, B.E. Conway, R.E. White (Eds.), Modern Aspects of Electrochemistry, vol. 22, Plenum Press, New York, 1992, p. 97.

[7] A. Bewick, S. Pons, in: R.J.H. Clark, R.E. Hester (Eds.), Advances in Infrared and Raman Spectroscopy, vol. 12, Wiley Hayden, Chichester, 1985, p. 1.

[8] T. Iwasita, F.C. Nart, in: W. Suetaka (Ed.), Surface Infrared and Raman Spectroscopy: Methods and Applications, Plenum Press, New York, 1995, p. 126.

[9] S.G. Sun, in: J. Lipkowski, P.N. Ross (Eds.), Electrocatalysis, Wiley-VCH, New York, 1998, p. 243.

[10] M. Fleischmann, P.J. Hendra, A.J. Mcquillan, Chem. Phys. Lett. 26 (1974) 163.

[11] D.L. Jeanmaire, R.P. Van Duyne, J. Electroanal. Chem. 84 (1977) 1.

[12] M.G. Albrecht, J.A. Creighton, J. Am. Chem. Soc. 99 (1977) 5212.

[13] R.K. Chang, T.E. Futak, Surface Enhanced Raman Scattering, Plenum Press, New York, 1982.

[14] J.E. Pemberton, in: H.D. Abruna (Ed.), In situ Studies of Electrochemical Interfaces: A Prospectus, VCH Verlag Chemie, Berlin, 1991, p. 328.
[15] B. Pettinger, in: J. Lipkowski, P.N. Ross (Eds.), Adsorption of Molecules at Metal Electrodes, VCH, New York, 1992, p. 285.
[16] G. Mengoli, M.M. Musiani, M. Fleischmann, B.W. Mao, Z.Q. Tian, Electrochim. Acta 32 (1987) 1239.
[17] J. Uehara, K. Aramaki, J. Electrochem. Soc. 138 (1991) 3245.
[18] K. Aramaki, M. Ohi, J. Uehara, J. Electrochem. Soc. 139 (1992) 1525.
[19] J. Gui, T.M. Devine, J. Electrochem. Soc. 138 (1991) 1376.
[20] C.A. Melendres, M. Pankuch, Y.S. Li, R.L. Knight, Electrochim. Acta 37 (1992) 2747.
[21] J.C. Rubim, J. Dunnwald, J. Electroanal. Chem. 258 (1989) 327.
[22] J.S. Gao, Z.Q. Tian, Spectrochim. Acta A 53 (1997) 1595.
[23] Z.Q. Tian, J.S. Gao, X.Q. Li, B. Ren, Q.J. Huang, W.B. Cai, F.M. Liu, B.W. Mao, J. Raman Spectrosc. 29 (1998) 703.
[24] S. Zou, C.T. Williams, E.K.Y. Chen, M.J. Weaver, J. Am. Chem. Soc. 120 (1998) 3812.
[25] S. Zou, M.J. Weaver, Anal. Chem. 70 (1998) 2387.
[26] S. Zou, M.J. Weaver, X.Q. Li, B. Ren, Z.Q. Tian, J. Phys. Chem. B 103 (1999) 4218.
[27] Z.Q. Tian, B. Ren, B.W. Mao, J. Phys. Chem. B 101 (1997) 1338.
[28] Q.J. Huang, X.Q. Li, J.L. Yao, B. Ren, W.B. Cai, B.W. Mao, Z.Q. Tian, Surf. Sci. 427/428 (1999) 162.
[29] P.G. Cao, J.L. Yao, B. Ren, B.W. Mao, R.A. Gu, Z.Q. Tian, Chem. Phys. Lett. 316 (2000) 1.
[30] D.Y. Wu, Y. Xie, B. Ren, J.W. Yan, B.W. Mao, Z.Q. Tian, Phys. Chem. Commun. 18 (2001) U1.
[31] Z.Q. Tian, B. Ren, Raman spectroscopy of electrode surfaces, Encyclopedia of Electrochemistry, Wiley-VCH, Volume Chapter 6, 2003.
[32] W.B. Cai, B. Ren, X.Q. Li, C.X. She, F.M. Liu, X.W. Cai, Z.Q. Tian, Surf. Sci. 406 (1998) 9.
[33] G. Xue, Y. Lu, G. Shi, Polymer 35 (1994) 2488.
[34] J. Rubim, I.G.R. Gutz, O. Sala, W.J. Orville-Thomas, J. Mol. Struct. 100 (1983) 571.
[35] R. Youda, H. Nishihara, K. Aramaki, Corros. Sci. 28 (1988) 87.
[36] D. Tromans, R. Sun, J. Electrochem. Soc. 138 (1991) 3235.
[37] H. Luo, Y.C. Guan, K.N. Han, Corrosion 54 (1998) 9.
[38] D.P. Schweinsberg, S.E. Bottle, V. Otieno-Alego, J. Appl. Electrochem. 27 (1997) 161.
[39] G.A. Hope, D.P. Schweinsberg, P.M. Fredericks, Spectrochim. Acta A 50 (1994) 2019.
[40] Y.C. Wu, P. Zhang, H.W. Pickering, D.L. Allara, J. Electrochem. Soc. 140 (1993) 2791.